Proceedings of the ASME 2010 Pressure Vessels & Piping Division / K-PVP Conference
PVP2010
July 18-22, 2010, Bellevue, Washington, USA

PVP2010-25806

THE COMPUTATION OF ACCURATE BUCKLING PRESSURES OF IMPERFECT THIN-WALLED CYLINDERS

Caitríona de Paor*
Department of Civil and
Environmental Engineering
University College Cork
Cork
Ireland
Email: c.depaor@student.ucc.ie

Denis Kelliher
Department of Civil and
Environmental Engineering
University College Cork
Cork
Ireland

Kevin Cronin
Department of Process and
Chemical Engineering
University College Cork
Cork
Ireland

William M.D. Wright
Department of Electrical and
Electronic Engineering
University College Cork
Cork
Ireland

ABSTRACT

The buckling capacity of thin cylindrical shells subject to uniform external pressure is investigated in this paper. Thin cylindrical shells are known to be highly sensitive to geometric and material imperfections such as wall thickness variation, non-circularity and random geometric imperfections. The effect of imperfection on the buckling load is studied using finite element (FE) models and laboratory experiments. Imperfection measurements are taken on small scale steel cans and these measurements are modelled and analysed using a geometrically non-linear static finite element analysis. The cans are then tested in the laboratory and the results compared with those predicted by the FE models and theory.

Keywords: Thin shells; Buckling; Geometric imperfections; Uniform external pressure

*Address all correspondence to this author.

NOMENCLATURE

E Young's Modulus.
Pc Critical buckling pressure.
l Length of shell.
n Number of circumferential buckling waves.
r Shell radius.
t Shell thickness.
μ Poisson's Ratio.

INTRODUCTION

Thin-walled cylindrical tanks common in the food and biotechnology sectors are prone to buckling collapse due to accidentally induced internal vacuum. Steam, used for sterilisation, can condense, and in turn, can cause the rapid development of this mode of failure. Such a collapse, if it occurs, tends to be catastrophic resulting in the complete destruction of the vessel. Notwithstanding that the basis of this type of failure is under-

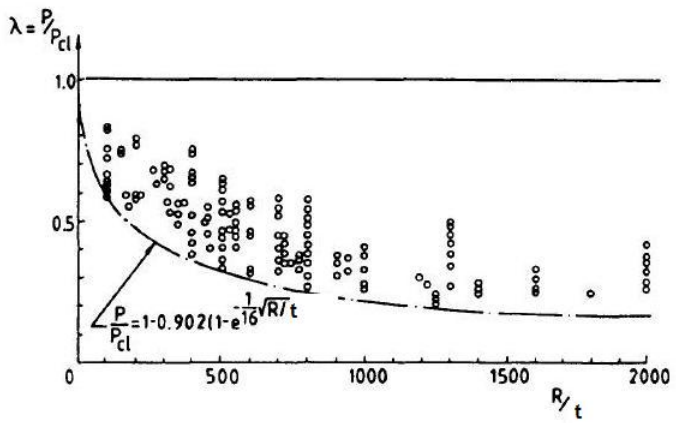

FIGURE 1. DISTRIBUTION OF BUCKLING TEST DATA FOR CYILNDERS WITH CLOSED ENDS SUBJECTED TO AXIAL COMPRESSION, FROM BRUSH AND ALMROTH [14]

stood and can generally be averted, it is still a regular occurrence, often due to the inadvertent closure of a safety release valve during sterilisation.

Buckling load calculations are seen to be one of the most challenging of analysis problems and since the beginning of the twentieth century, much research has been published in this area [1–5]. Early experimental studies showed that cylindrical shells subjected to uniform external pressure collapse at loads significantly lower than those predicted by classical buckling theory. Shell buckling has been found to occur at loads between 10% and 80% of the theoretical buckling load. Figure1 represents values for the experimental buckling pressure P, divided by the theoretical buckling pressure Pcl, versus the radius/thickness ratio. Since the buckling load is dependent on the geometry of the shell, most importantly the L/r (length to radius) and t/r (thickness to radius) ratios, it is widely accepted that these discrepancies are due to the highly sensitive nature of the shells to geometric and material imperfections [6]. Geometric imperfections such as out-of-roundness, wall thickness variation and random geometric imperfections, as well as material imperfections such as anisotropy, all greatly reduce the buckling capacity of shells. Some studies have investigated the effect of geometric imperfections on buckling capacity either experimentally [7–9] or numerically [10, 11] but few have compared experimental results to a nonlinear Finite Element (FE) analysis which includes the geometric imperfections [12, 13].

An Initial Imperfection Data Bank [3] was set up in the 1980s containing results of several imperfection surveys of shells. Researchers could contribute their own data or use the data in numerical analysis with the aim of improving design standards. This led to several studies on the effect of initial imperfection on buckling capacity including analysis on shells subjected to axial loading [15–17]. Studies on other geometric imperfections have also been carried out such as variation in shell thickness investigated by Aghajari et al. [5], the effect of presence of a dent in addition to initial imperfection on the buckling capacity carried out by W. Guggenburger [18] and Park and Kyriakides [19], and the influence of welds on buckling capacity examined by J.G. Teng [20].

Sophisticated methods of nonlinear analysis that allow the user to include for these imperfections exist for this type of problem but the difficulty of accurate buckling load prediction persists. This study focuses on the effect of manufacturing-induced geometric imperfections on the buckling of thin cylindrical shells under uniform vacuum. The geometric imperfections of small-scale steel cans are measured and subsequently modelled in FE. These cans are then tested in the laboratory with the results compared to those predicted by the FE analysis.

BUCKLING THEORY

Buckling is one of the most complex structural analysis problems and buckling loads remain difficult to accurately predict. A combination of axial loads and external pressure is typical in machine design, ship building or tanks used in chemical engineering. If a cylinder is loaded with a uniform hydrostatic pressure such as this, a bifurcation point will be reached where the net external pressure on the vessel exceeds a critical pressure, Pc. At this point, sudden or 'snap-through' radial buckling will occur. There are a number of approaches to obtain values for Pc; the most frequently used being the equilibrium method. The equilibrium method is based on the observation that at a critical load, a deformed state of a shell exists that is assumed to be close to its initial unbuckled state of equilibrium. Thus the appearance of a possible bifurcation in the solution corresponds to the critical load. This criterion for determining critical loads can be used to obtain the governing differential equations of the shell buckling analysis [21]. This method may be employed when an axial load is present in addition to external lateral pressure, as in this case. Von Mises [4] solved this for a cylindrical shell with closed end subjected to the action of a uniform hydrostatic pressure obtaining the following expression:

$$Pc = \frac{Et}{r}\left(\frac{1}{n^2+\frac{1}{2}(\frac{\pi r}{l})^2}\right) \left(\frac{1}{(n^2(\frac{l}{\pi r})^2+1)^2}+\frac{t^2}{12(1-\nu^2)r^2}\left(n^2+(\frac{\pi r}{l})^2\right)^2\right) \quad (1)$$

As can be seen from Eqn. (1), the critical buckling pressure is primarily dependent on the vessel geometry, and in particular, the t/r ratio. It is also directly proportional to the Young's Modulus of the material. The critical pressure is also dependent on

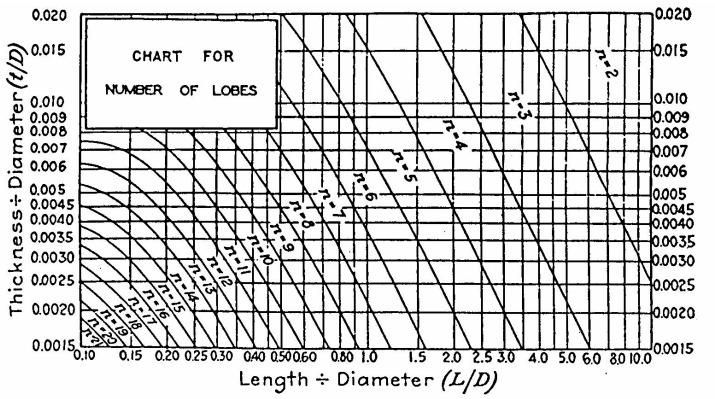

FIG. 1 NUMBER OF LOBES n INTO WHICH A SHELL WILL COLLAPSE WHEN SUBJECTED TO UNIFORM COLLAPSING PRESSURE ON SIDES AND ENDS

FIGURE 2. CHART FOR NUMBER OF LOBES

the number of circumferential half-waves, n, formed during the buckling process, with a minimum buckling pressure occurring at a specific value of n. n is dependent on vessel geometry, and can be taken from the chart in Fig. 2 developed by D.F. Windenburg and C. Trilling [22]. It is evident from the chart that the number of circumferential waves which form as the shell buckles increases as the length and thickness of the shell decrease. The value of n may also be calculated as the value which gives a minimum for P_c.

IMPERFECTION MEASUREMENT

To model real geometric imperfections precisely and accurately, measurements of 39 small-scale steel cans were recorded using a custom-built rig. The can walls were cut from rolled steel, welded together with a seam and the ends added on with a method of folding. They contain imperfections typical of those caused inadvertently by the manufacturing process and so are suitable for this study. The cans were centred and secured on a base plate which rotated 360°, and four dial gauges, accurate to $\pm$ 5 μm, moved vertically on linear actuators. Three of the dial gauges (No. 1, 2 and 3) were positioned at 120° intervals outside the can with the fourth on the interior, directly opposite gauge No. 1. The base plate was rotated at 2.5° intervals, and after each complete rotation of 360°, the sensors moved vertically downwards in increments of 5 mm. This procedure was repeated until the entire surface area of the can had been measured with a total of 5760 measurements per can. In this manner, full geometric information including the thickness variation for each can is produced. Figure 3 shows the measurement rig set-up.

Imperfection in the measurement rig could not be measured a priori. Therefore the measurement redundancy was used to determine the systemic errors in the testing rig. Two sensors would have been adequate to record the surface and thickness imperfections; however the extra sensor readings were used to eliminate these systemic errors from the data. Firstly, the actuators did not move exactly parallel to the can wall distorting the data which was evident on comparison of measurements from different gauges. Also, the positioning of the centre of the can on the base plate produced an error since it was not exactly on the centre of rotation of the base plate. Once these errors were evaluated and quantified numerically, the data was corrected accordingly. Figures 4 to 8 show the surface plots generated in MATLAB for each of the five cans used in testing. These were then used to generate FE models.

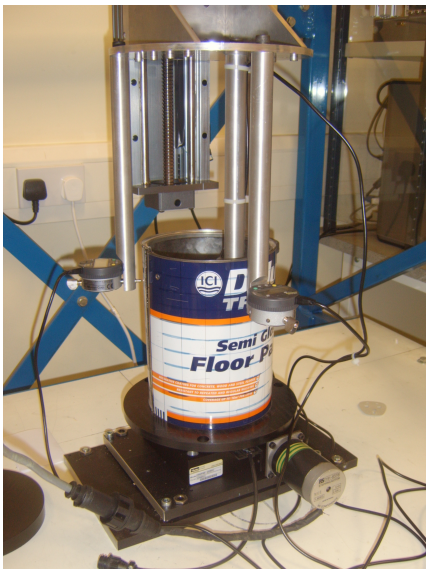

FIGURE 3. CAN MEASUREMENT RIG.

The thickness variation around the can was also investigated. This was done using the readings from gauge No. 1 and gauge No. 4. Since the gauges were directly opposed, the thickness variation could be evaluated as the difference in readings at each point. Figure 9 shows this for Can 17. A regression analysis was carried out on the thickness variation and it was found to vary quadratically with the thinnest region near the position of the weld, and the thickest region directly opposite this at 180°. The thickness variation between the maximum and minimum points was found to be about 10 μm. This variation was modelled in the FE analysis.

NUMERICAL ANALYSIS

In order to determine the buckling pressure of these imperfect shells, finite element analysis is carried out using the corrected data from the imperfection measurements. The general-purpose finite element analysis system Strand7 is used. The model mesh was set up with approximately one node for each reading taken on the can. Rectangular 9-noded quadrilateral shell elements based on Kirchoff's plate theory were used with 6 de-

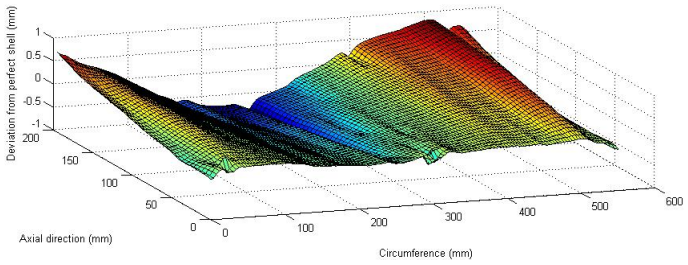

FIGURE 4. SURFACE PLOT OF CAN 12

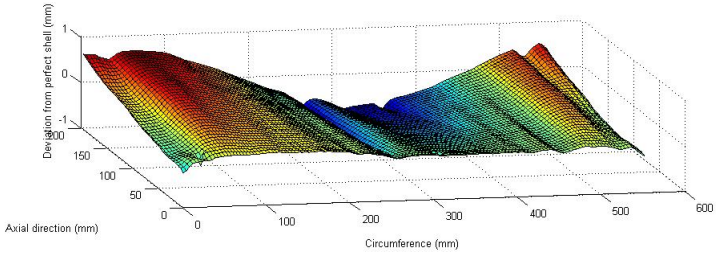

FIGURE 5. SURFACE PLOT OF CAN 17

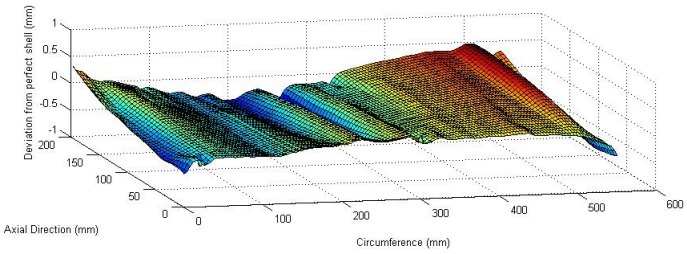

FIGURE 6. SURFACE PLOT OF CAN 24

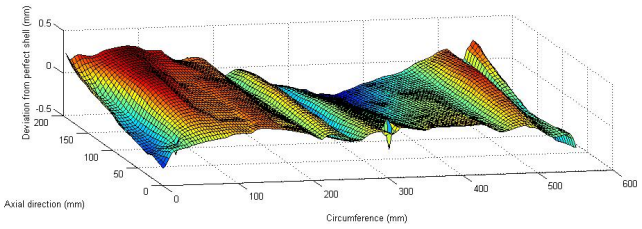

FIGURE 7. SURFACE PLOT OF CAN 28

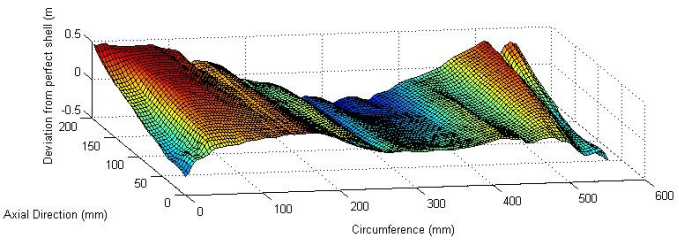

FIGURE 8. SURFACE PLOT OF CAN 35

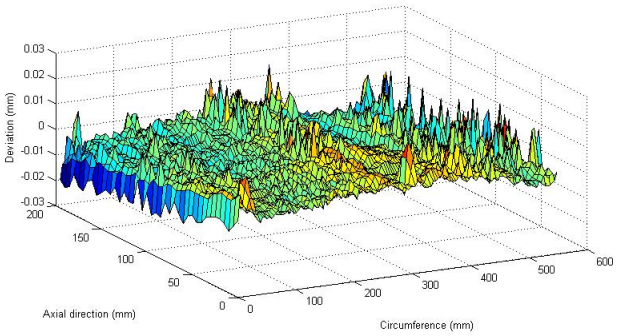

FIGURE 9. THICKNESS VARIATION OF CAN 17

TABLE 1. NOMINAL CAN DIMENSIONS, GIVEN IN mm.

Height	Thickness	Radius
230	0.22	88.2

grees of freedom at each node; 3 translational and 3 rotational. These 9-noded quadrilateral shell elements were chosen for their accuracy in representing the curved geometry of the shell. Each side is a quadratic curve in XYZ-space (like a parabola) defined by the three points on that side. This makes it a suitable element for representing curvature. Translation in the axial (Z) direction was prevented by restraining the nodes at the bottom of the can where the can wall meets the base at z = 0 and R = r. In addition, translation of one of these nodes was restrained in the X and Y direction and in another node in just the Y direction to ensure no rigid body movement.

Tensile tests were carried out on several samples of material from previously collapsed cans to establish the tensile strength of the material. The Young's Modulus was found to be 205 GPa. This is assumed constant over the temperature range of the experiment. Dimensions of the can are modelled based on measurements taken shown in Tab. 1. These values represent nominal dimensions for a perfect shell. The longitudinal welded seam on the can was modelled using a three-node beam element with 6 degrees of freedom at each node; 3 translational and 3 rotational. This element can be used to define quadratic geometry and is suited for large rotations and large displacement nonlinear analysis. The material properties of the weld are similar to those of the can wall. The width of the beam is found to be 0.4mm. The thickness of the seam is found to be twice the thickness of the can wall, 0.44mm. The FE model is shown in Fig. 10. Plates were modelled with a thickness variation as shown in Fig. 9 also based on the measured data.

FE models replicating the real cans were thus generated and geometrically non-linear analyses were carried out to determine

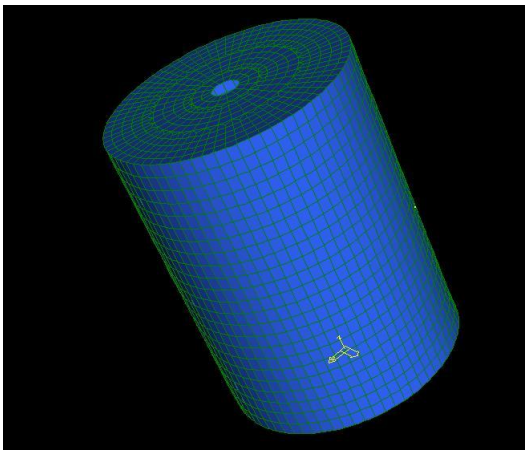

FIGURE 10. FE MODEL OF CAN

FIGURE 11. EXPERIMENTAL SET-UP WITH CAN IN PLACE

the buckling pressures. The nonlinear analysis uses the Arc Length Method. In this method, the load is applied incrementally and the arc length method searches along the equilibrium path, allowing movement forward up to a specified amount that is a balance of load and displacement in the increment.

EXPERIMENTAL ANALYSIS

To validate the FE analysis, five of the measured cans were tested in the laboratory. Each can in the whole collection was assigned a number in the range 1-39. The cans to be tested were chosen at random from the collection and were numbered 12, 17, 24, 28 and 35. Dimensions are given in Tab. 1. The experimental set-up is as shown in Fig. 11. The cans were simply supported with closed ends. Steam at 100°C flowed in one end pushing out cooler air through an outlet pipe at the other end. At each end was a valve and when the can had been filled with steam and the cooler air emptied, the valves were closed. The cans were allowed cool under normal atmospheric conditions. Upon cooling, the steam inside the vessel condensed, creating a uniform vacuum (negative pressure), causing buckling and ultimately the complete collapse of the vessel. Pressure is recorded throughout

TABLE 2. ANALYTICAL, NUMERICAL AND EXPERIMENTAL RESULTS

Can	Analytical kPa	FE Analysis kPa	Experimental kPa	% difference (FE - Exp.)
24	23.17	22.2	19.93	11.4
28	23.17	21.7	20.31	6.8
17	23.17	22.2	20.86	6.4
35	23.17	24.0	21.37	12.3
12	23.17	23.2	21.70	6.9
Mean	23.17	22.7	20.83	

the experiment using a pressure sensor located inside the can as well as one outside recording ambient pressure. The experimental collapse pressure given in Tab. 2 is calculated as the difference between the two recorded measurements.

RESULTS

Table 2 contains the theoretical results from the Von Mises formula for the buckling of a perfect cylinder subjected to uniform external pressure. The numerical and experimental values for critical pressure for each of the five cans are also presented here. The number of circumferential waves, n, predicted by both analytical and numerical analyses is 8 for each of the cans. In the experiments, six circumferential waves are clearly visible. Figure 12 displays the buckled shape predicted by the FE model. Figure 13 shows the deformed shape of the can after testing. Figure 14 shows the force-displacement curve for all cans. The displacement shown in this graph is the radial displacement of the node where the greatest deformation occurs.

DISCUSSION

On comparing the buckling pressures attained by experiment with those predicted by the FE analysis(see Tab. 2), good correlation is shown. For three of the cans, buckling pressures are within 7% and for the other two, around 12%. These results are consistent with those found in the literature. Aghajari et al. [5] presented an error of 7-13% between numerical and experimental results, Frano and Forasassi [13] achieved results within 10-15% and Reid et al. [12] presented results with a discrepancy of about 10%. The numerical analysis overestimates the experimental collapse pressure for each can. This is also consistent with previous research [5, 12, 13]. Discrepancies of up to 17% exist between

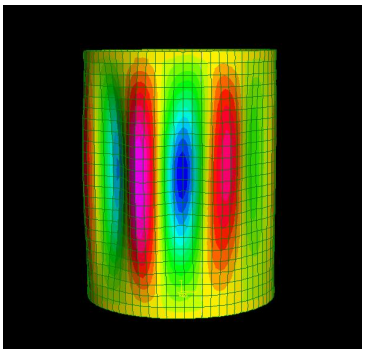

FIGURE 12. BUCKLED SHAPE PREDICTED BY FE ANALYSIS

FIGURE 13. DEFORMED CAN AFTER TESTING

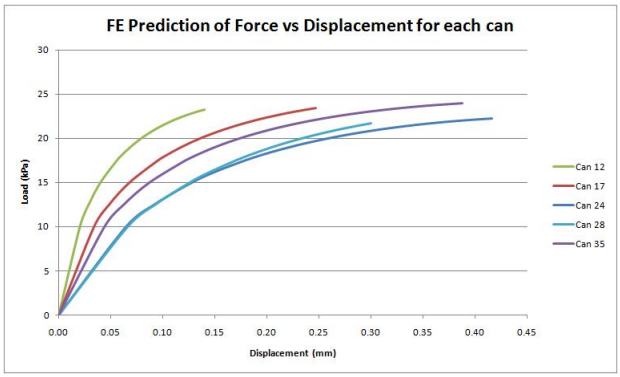

FIGURE 14. FORCE DISPLACEMENT CURVE FOR ALL CANS

the classical theory prediction of the buckling load and the experimental results. This inconsistency may be attributed to the sensitivity of the experimental buckling loads to imperfection. The classical theory is based on the assumption of a perfect shell and so will give more conservative results than experimental results. The number of circumferential waves of $n = 8$ is predicted both by the theory and FE models. These values are higher than the value of $n = 6$ noted in the experiments. One explanation for this could be that the can in the experiments buckled elastically with initial shape of $n = 8$ but this deformation was not visible to the human eye. On entering postbuckling, this was reduced to $n = 6$. This occurrence was described by Hornung and Saal [23] and Guggenburger [18] but has not yet been fully explained. Capturing the buckling process on high-resolution camera may lead to confirmation of this.

CONCLUSION

An experimental and numerical analysis of the buckling of cylindrical shells under a uniform external loading is presented. Geometric imperfections based on measured data of five cans were modelled in a nonlinear finite element analysis. Buckling collapse experiments were carried out in the laboratory and the results compared. The study shows that the numerical analysis of the buckling process predicted by the FE model closely follows the experimental behaviour. Despite the structural complexity of the buckling phenomenon buckling behaviour can be satisfactorily predicted using finite element analyses when nonlinearity of the model is taken into account.

ACKNOWLEDGMENT

Thanks go to Paul Conway who helped with the experimental setup, Tim Power and Michael O'Shea who very carefully built the measurement rig, and Sean McSweeney who helped with the imperfection measurement. Funding for this research was provided by IRCSET Embark Initiative.

REFERENCES

[1] Southwell, R., 1914. "On the general theory of elastic stability". *Phil Trans Roy Soc London Ser A,* ***213***, pp. 187–244.

[2] Timoshenko, S. P., and Gere, J. M., 1963. *Theory of Elastic Stability*, 2 ed. McGraw-Hill Book Company.

[3] Arbocz, J., and Abramovich, H., December 1979. The initial imperfection data bank at the delft university of technology, part 1. Tech. Rep. LR-290, Delft University of Technology, Department of Aerospace Engineering.

[4] Allen, H. G., and Bulson, P., 1980. *Background to Buckling*. McGraw-Hill Book Company Limited.

[5] Aghajari, S., Abedi, K., and Showkati, H., 2006. "Buckling and post-buckling behavior of thin-walled cylindrical steel shells with varying thickness subjected to uniform external pressure". *Thin-Walled Structures,* ***44***(8), pp. 904–909.

[6] Koite, W., 1963. "The effect of axisymmetric imperfections on the buckling of cylindrical shells under axial compression". *roceedings Koninklijke Nederlandse Akademie van Wetenschappen*, pp. 265–279.

[7] Lundquist, E. E., 1933. Strength tests of thin-walled duralumin cylinders in compression. Tech. Rep. TR-473, NACA.
[8] Wilson, W. M., and Newmark, N. M., 1933. The strength of thin cylindrical shells as columns. Tech. rep., The Engineering Experiment Station, University of Illinois.
[9] Almroth, B., Holmes, A., and Brush, D., 1964. "An experimental study of the buckling of cylinders under axial compression". *Experimental Mechanics,* ***4***, pp. 263–270.
[10] Vodenitcharova, T., and Ansourian, P., 1996. "Buckling of circular cylindrical shells subject to uniform lateral pressure". *Engineering Structures,* ***18***, pp. 604–614.
[11] Khamlichi, A., Bezzazi, M., and Limam, A., 2004. "Buckling of elastic cylindrical shells considering the effect of localized axisymmetric imperfections". *Thin-Walled Structures,* ***42***, pp. 1035–1047.
[12] Reid, J. D., Bielenberg, R. W., and Coon, B. A., 2001. "Indenting, buckling and piercing of aluminum beverage cans". *Finite Elements in Analysis and Design,* ***37***, pp. 131–144.
[13] Frano, R. L., and Forasassi, G., 2009. "Experimental evidence of imperfection influence on the buckling of thin cylindrical shell under uniform external pressure". *Nuclear Engineering and Design,* ***239***, pp. 193–200.
[14] Arbocz, J., and Hol, J., 1995. "Collapse of axially compressed cylindrical shells with random imperfections". *Thin-Walled Structures,* ***23***, pp. 131–158.
[15] Schenk, C., and Schuëller, G., 2003. "Buckling analysis of cylindrical shells with random geometric imperfections". *International Journal of Non-Linear Mechanics,* ***38***, pp. 1119–1132.
[16] Arbocz, J., 1984. "Collapse load calculations for axially compressed imperfect stringer stiffened shells". In Proceedings of AIAA/ASME/ASCE/AHS 25th SDM Conference, Part 1, pp. 130–139.
[17] Elishakoff, I., and Arbocz, J., 1982. "Reliability of axially compressed cylindrical shells with random axisymmetric imperfections". *International Journal of Solids and Structures,* ***18***, pp. 563–585.
[18] Guggenburger, W., 1995. "Buckling and postbuckling of imperfect cylindrical shells under external pressure". *Thin-Walled Structures,* ***23***, pp. 351–366.
[19] Park, T., and Kyriakides, S., 1996. "On the collapse of dented cylinders under external pressure". *Int. J. Mech. Sci,* ***38***, pp. 557–578.
[20] Teng, J., and Lin, X., 2005. "Fabrication of small models of large cylinders with extensive welding for buckling experiments". *Thin-Walled Structures,* ***43***, pp. 1091–1114.
[21] Ventsel, E., and Krauthammer, T., 2001. *Thin Plates and Shells*, 1 ed. Marcel Dekker Inc.
[22] Windenburg, D. F., and Trilling, C., 1934. "Collapse by instability of thin cylindrical shells under external pressure". *Trans. ASME,* ***56***, pp. 819–825.
[23] Hornung, U., and Saal, H., 2002. "Buckling loads of tank shells with imperfections". *International Journal of Non-Linear Mechanics,* ***37***, pp. 605–621.